Supporting Information for:

Charge localization, stabilization and hopping in lead-halide perovskites: Competition between polaron stabilization and cation disorder

Francesco Ambrosio,[a,b,]* Daniele Meggiolaro,[a,b] Edoardo Mosconi,[a,b] Filippo De Angelis[a,b,c]*

[a]*Computational Laboratory for Hybrid/Organic Photovoltaics (CLHYO), Istituto CNR di Scienze e Tecnologie Molecolari (ISTM-CNR), Via Elce di Sotto 8, 06123 Perugia, Italy*

[b]*CompuNet, Istituto Italiano di Tecnologia, Via Morego 30, 16163 Genova, Italy*

[c]*Department of Chemistry, Biology and Biotechnology, University of Perugia, Via Elce di Sotto 8, 06123 Perugia, Italy*

*E-mail: Francesco.Ambrosio@iit.it, filippo@thch.unipg.it

1. Polaron binding energy vs. Fock exchange

To calculate the energy levels of polarons and defects in $CH_3NH_3PbI_3$, we adopt the grand-canonical formulation of defects in crystalline materials.[1, 2] In this formulation, the formation energy of a defect with charge q, $E_f^q[X]$, is expressed as a function of the electron chemical potential μ:

$$E_f^q[X] = E^q[X] - E[\text{bulk}] - \sum_i n_i \mu_i + q(\varepsilon_V + \mu) + E_{\text{corr}}^q, \tag{1}$$

where $E^q[X]$ is the total energy of the defect X in the charge state q, $E[\text{bulk}]$ is the total energy of the pristine bulk system, μ_i is the chemical potential of the subtracted/added species i, ε_V the valence band edge of the pristine system, and E_{corr}^q is a correction term which accounts for electrostatic finite-size effects. The charge transition level $\mu(q/q')$ is defined as the electron

chemical potential for which the formation energies of a defect X in the charge states q and q' are equal $(E_f^q[X] = E_f^{q'}[X])$. This results in the following expression:

$$\mu(q/q') = \frac{E^q[X] - E^{q'}[X]}{q' - q} + \frac{E_{corr}^q - E_{corr}^{q'}}{q' - q} - \varepsilon_V. \tag{2}$$

For the localization of the hole, we can write the following reaction:

$$CH_3NH_3PbI_3 + h^+ \longrightarrow h_{loc}. \tag{3}$$

The hole polaron level can then be defined as follows:

$$\mu(h_{loc}) = E[h_{loc}] - E[CH_3NH_3PbI_3] + E_{corr}^{+1} - \varepsilon_V, \tag{4}$$

where $E[h_{loc}]$ is the total energy of the hole polaron and $E[CH_3NH_3PbI_3]$ the total energy of the pristine perovskite. Analogously, we can write the following reaction for the extra electron:
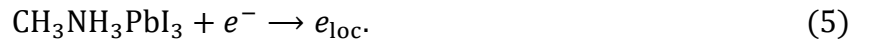
$$CH_3NH_3PbI_3 + e^- \longrightarrow e_{loc}. \tag{5}$$

The respective charge transition level is then given by:

$$\mu(e_{loc}) = E[e_{loc}] - E[CH_3NH_3PbI_3] + E_{corr}^{-1} - \varepsilon_V, \tag{6}$$

where $E[e_{loc}]$ is the total energy of the electron polaron. In order to achieve values referred to the respective band edge for both the hole and the electron polaron, we define the polaron binding energies as $E_b(h^+) = \mu(h_{loc})$ and $E_b(e^-) = \varepsilon_C - \mu(e_{loc})$ where ε_C is the conduction band edge of pristine CH_3PbI_3. We remark that electrostatic finite size corrections are here taken into account, using the Freysoldt-Neugebauer-Van de Walle (FNV) scheme.[1, 3] Two terms are included in the FNV scheme: (i) the Madelung energy, that correct the interaction of a charge with its periodic replica, and (ii) an alignment-like term that takes into account the finite extent of the charge distribution. The calculated correction for the 2×2×2 supercell CH_3PbI_3 considered in this work amounts to 0.01 eV and is therefore negligible.

In order to evaluate the polaron binding energy as a function of Fock exchange, we perform density functional theory calculations on model **3**, as defined in the main text. We first employ the PBE0 functional[4, 5] with the fraction of Fock exchange α set to the standard value of 0.25, as this value has proved to comply the Koopman condition[6] for this material.[7] We obtain polaron formation upon structural relaxation (cf. main text) with binding energies of 0.09 eV and 0.06 eV for the localized hole and electron, respectively. Next, we keep the bulk and polaronic structure fixed and we recalculate the total-energy differences of Eqs. (4) and (5), performing (i) PBE0 calculations with two different values for the fraction of Fock exchange α (0.35 and 0.45) and (ii) calculations at the semi-local PBE level of theory.[8] The calculated defect levels, aligned through the average electrostatic potential, are reported in Fig. S1 as a function of the fraction of Fock exchange introduced in the functional. $\mu(h_{\mathrm{loc}})$ and $e(h_{\mathrm{loc}})$ both show a constant behaviour, except for the PBE values ($\alpha = 0$) for which the polaron binding energy almost vanishes. This behaviour is typically observed for charge transition levels of defects in crystalline materials and redox levels in aqueous solution.[9-12] However, while $\mu(h_{\mathrm{loc}})$ and $e(h_{\mathrm{loc}})$, remain constant with α, the valence (conduction) band edge moves to lower (higher) energies linearly.[13] Therefore, for large values of α, polaron levels are found to be more detached from the respective band edge, a result contrasting with available measurements[14] and previous theoretical estimates.[28] At variance, at the PBE level, polaronic structures are found to be only marginally stabilized, as calculated binding energies are below 10 meV. Therefore, the present results indicate the particular care should be devoted when choosing a functional to study the energetics of polarons. In this regard, the choice of a Koopman compliant hybrid functional has proved to provide excellent results in the accurate determination of band gaps and defect levels for semiconductors and insulators.[15, 16]
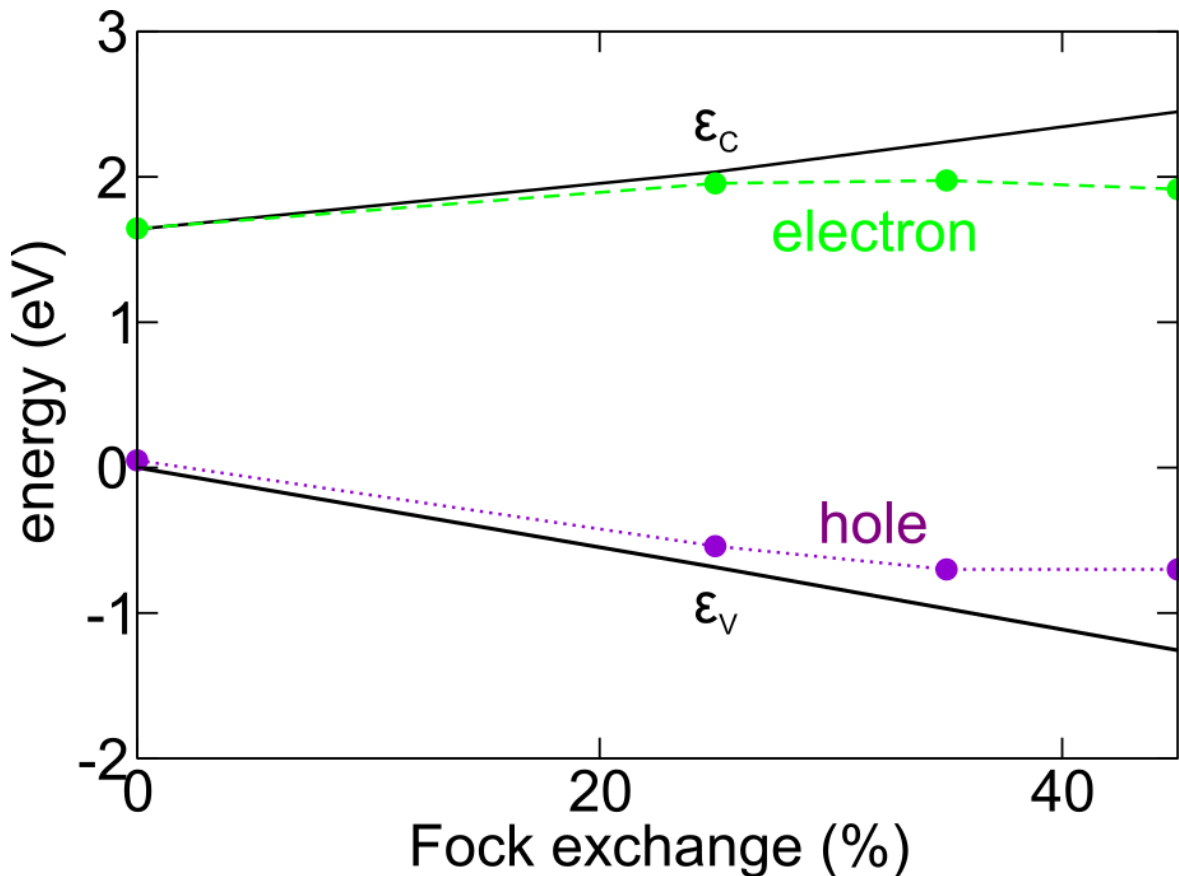
Figure S1. $\mu(h_{loc})$ (purple dotted) and $\mu(e_{loc})$ (green dashed) the fraction α of Fock exchange, aligned through the average electrostatic potential and referred to the VBM calculated at the PBE level (α = 0); ε_V and ε_C are also reported as solid black lines.

2. Benchmark of supercell size

In order to check the accuracy of our approach, we calculate E_s^+ (cf. main text) for supercells of (i)

larger size and (ii) different shapes. These calculations are performed for the three different models

described in the main text. Results are reported in Table S1. For structural model **1**, the difference in

the calculated values of E_s^+ is negligible (8 meV), when increasing the supercell size from 2×2×2 to

2×2×4. Since the charge in this model is essentially delocalized, we do not consider any other

supercell. In contrast, for structural model **2**, we consider 2×2×4, 2×2×6, 2×2×8, and 4×4×4

supercells and we calculate E_s^+ ranging from 54 meV to 197 meV, with an average of 142 meV, in

line with the value reported in the main text. We note that the structures are constructed from

periodic replicas of a configuration achieved with a molecular dynamics simulation performed on

the $2\times2\times2$ supercell. Therefore, the small differences encountered might even reduce if employing structural configurations achieved from molecular dynamics for each supercell. Finally, we consider structural model **3** for which we observe a continuous increase of E_s^+ from the $2\times2\times2$ supercell to the $2\times2\times8$ one. Since this model has been artificially constructed to enhance charge separation, the calculated E_s^+ grows as the supercell size is increased along the tetragonal axis. However, we notice that, while E_s^+ becomes larger, so does the energy difference among neutral model **1** and **3**. In fact, since more methylammonium cations are artificially orientated, neutral model **3** becomes more energetically unfavourable and the increased E_s^+ does not compensate for it.

Table S1. Values of stabilization energies (meV) of the hole polaron calculated for different supercells of the considered structural models (cf. main text) of tetragonal $CH_3NH_3PbI_3$.

Supercell	Structure 1	Structure 2	Structure 3
2x2x2	13	140	110
2x2x4	20	54	174
2x2x6	-	197	238
2x2x8	-	192	331
4x4x4	-	132	-

3. Calculation of the energy barriers

The coordinates of the two neighbouring polaronic structures R_i and R_j are linearly interpolated[17] according to the following expression: $R_\lambda = \lambda R_i + (1 - \lambda)R_j$ where λ is the coupling parameter connecting the two models. For the hole polaron, we consider five intermediate values of λ (0.25, 0.375, 0,5, 0.675, 0.75), and three values (0.25, 0.5, 0.75) for the electron polaron. The achieved structures are then allowed to undergo structural relaxation in which the organic cations are free to relax. In contrast, the positions of the atoms belonging to the inorganic sub-lattice are fixed. In this

way, we avoid unstable and highly energetic structures due to linear interpolation of the coordinates of the freely-rotating organic cations. In order to test the accuracy of the employed method, we perform an additional nudge elastic band calculation (NEB) for the electron polaron. We consider the same initial and final model used for the linear transit calculation and we provide the structural configuration at $\lambda = 0.5$, as a starting guess of the intermediate structure. The calculation is carried out with the improved tangent (IT) method,[18] considering five replicas between the initial and final configurations. The energy barrier achieved with the NEB method is 110 meV, a value larger by only 20 meV than that calculated with the linear transit method reported in the main text, thus ensuring that the discussion is not affected by the use of a simplified computational protocol. Inspection of the wave-function of the saddle point confirms that the transition state is a band-like semi-localized state.

4. Time-evolution of $CH_3NH_3^+$ orientation for regular and "heavy" $CH_3NH_3PbI_3$

We here analyse the evolution of the $CH_3NH_3^+$ orientation during the molecular dynamics (MD) simulation in presence of an extra positive charge for (i) regular $CH_3NH_3PbI_3$ and (ii) for a system in which hydrogen atoms of the $CH_3NH_3^+$ cations are substituted with artificial isotopes of atomic mass equal to 12 atomic mass units. We consider the same $CH_3NH_3^+$ cation picked from structural model **1** and we follow the time-evolution of the of ϕ angle (cf. main text for definition) during the MD simulations for both system. The results shown in Fig. S2 clearly highlight the different behaviour of the normal and weighted cation. In fact, the former is found to undergo large fluctuations in the orientation, evidenced by the wide fluctuations of ϕ angle during the MD. At variance, only moderate fluctuations of the ϕ angle are observed for the weighted $CH_3NH_3^+$ cation. The same considerations are found to apply also for the θ angle (not shown).
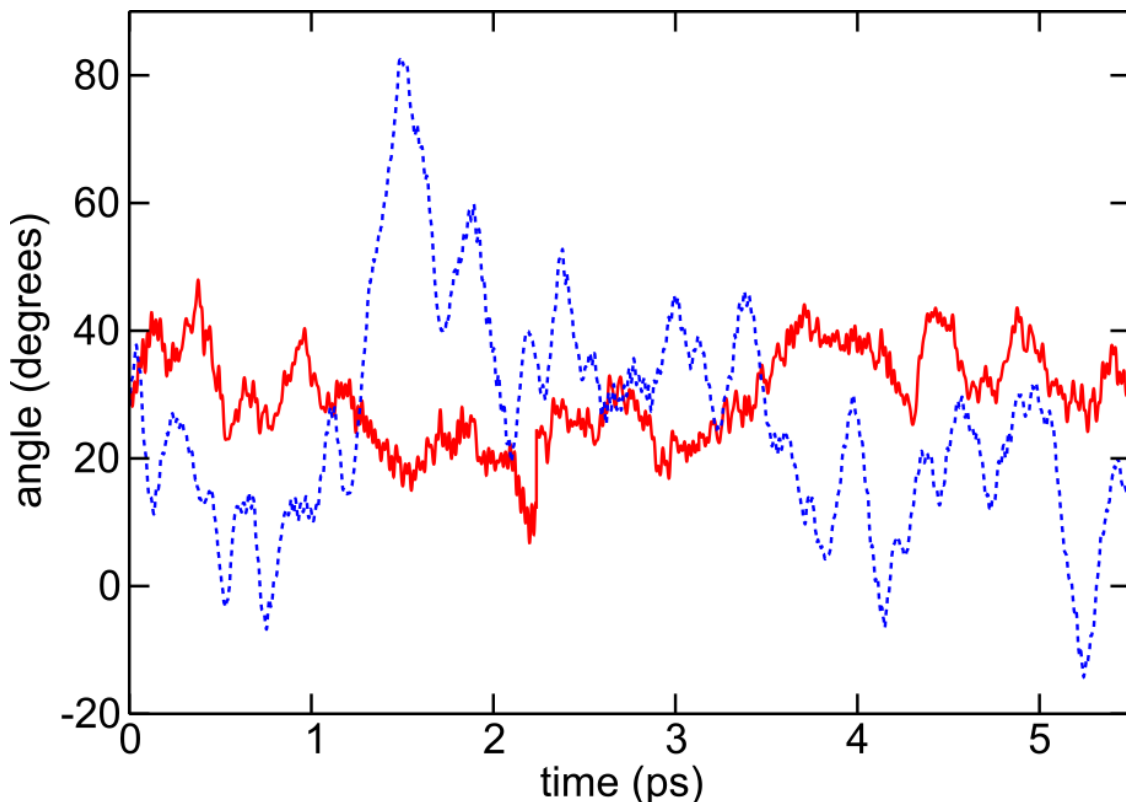
Figure S2. Time-evolution of the ϕ angle of regular (blue dotted) and "heavy"(red solid) $CH_3NH_3^+$ in $CH_3NH_3PbI_3$ for a selected $CH_3NH_3^+$ cation.

5.Time-dependent orientation of $CH_3NH_3^+$ in $CH_3NH_3PbI_3$ and of $CH(NH_2)_2^+$ in $CH(NH_2)_2PbI_3$

We here report on the comparison between the time-evolution of the orientation for $CH_3NH_3^+$ in $CH_3NH_3PbI_3$ and of $CH(NH_2)_2^+$ in $CH(NH_2)_2PbI_3$. For both systems, we carry out a molecular dynamics simulation of the neutral system at room temperature at the PBE level of theory.[8] The sampling of the *NVT* ensemble is ensured by the use of a Nosé-Hoover thermostat[18, 19] and simulations are carried out for 12 picoseconds. For $CH_3NH_3PbI_3$, we consider structural model **1** (cf. main text), as the starting point of the MD simulation. For $CH(NH_2)_2PbI_3$, we consider a 288-atoms 2×2×2 supercell at the experimental density.[20]

Then, we analyse the time-dependent orientation of the cations, by following the time-evolution of the average values for ϕ and ϕ angles. For the $CH(NH_2)_2^+$ cation, the angle ϕ is formed by the CH

7

axis with the *ab* plane and the angle θ is given by the projection of the CH axis on the *ab* plane and the *a* axis. The results depicted in Fig. S3 highlight a remarkable difference between $CH_3NH_3^+$ and $CH(NH_2)_2^+$, with the latter being capable of larger reorientations in a shorter time.

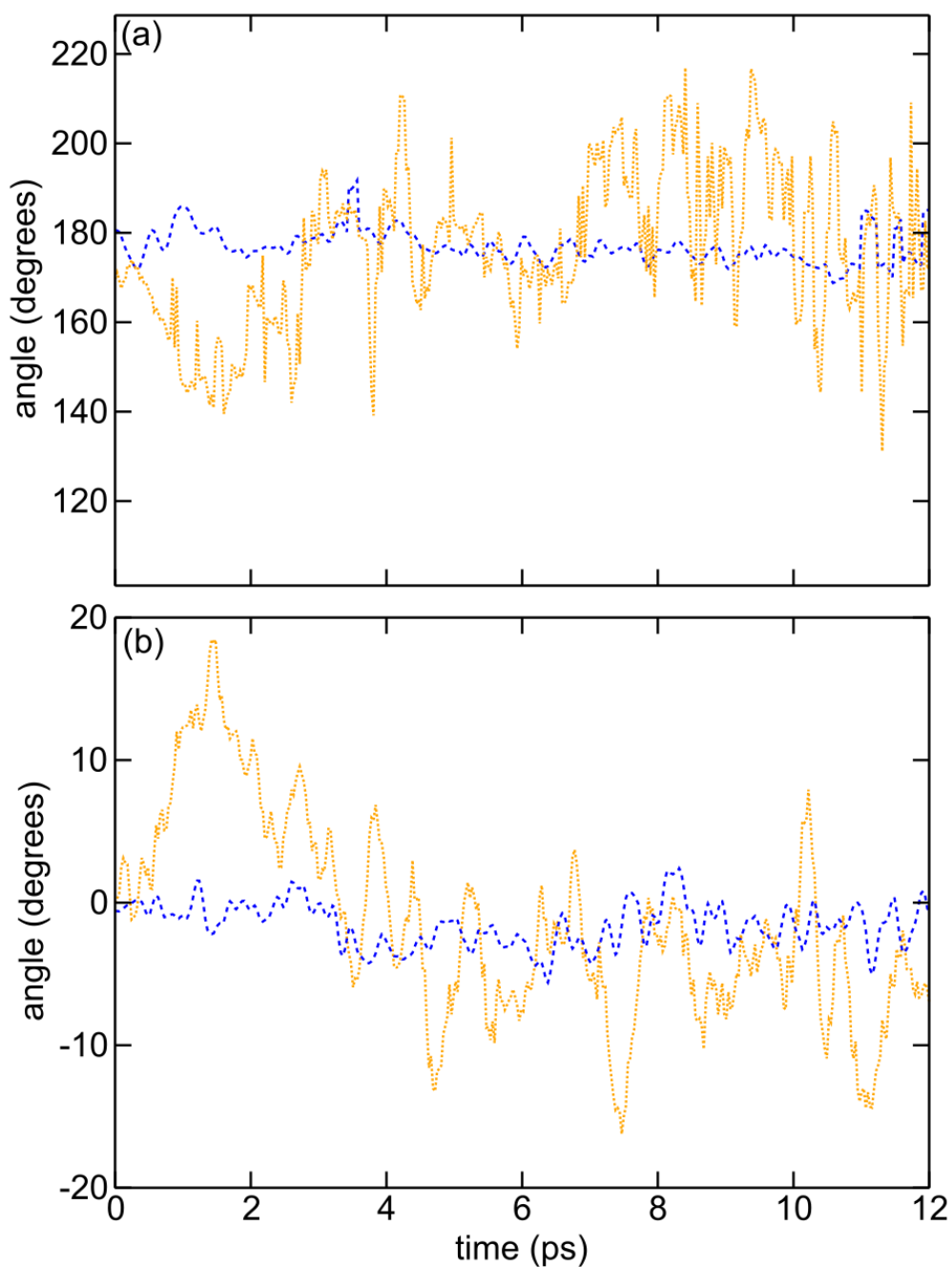**Figure S3.** Time-evolution of the average value of ϕ (a) and θ (b) angle for $CH_3NH_3^+$ in $CH_3NH_3PbI_3$ (blue dashed lines) and $CH(NH_2)_2^+$ in $CH(NH_2)_2PbI_3$ (orange dotted).

References

1.   Komsa, H.-P.; Rantala, T. T.; Pasquarello, A., Finite-Size Supercell Correction Schemes for Charged Defect Calculations. *Physical Review B* **2012,** *86* (4), 045112.

2.   Freysoldt, C.; Grabowski, B.; Hickel, T.; Neugebauer, J.; Kresse, G.; Janotti, A.; Van de Walle, C. G., First-Principles Calculations for Point Defects in Solids. *Reviews of Modern Physics* **2014,** *86* (1), 253-305.

3.   Freysoldt, C.; Neugebauer, J.; Van de Walle, C. G., Fully Ab Initio Finite-Size Corrections for Charged-Defect Supercell Calculations. *Physical Review Letters* **2009,** *102* (1), 016402.

4.   Perdew, J. P.; Ernzerhof, M.; Burke, K., Rationale for Mixing Exact Exchange with Density Functional Approximations. *The Journal of chemical physics* **1996,** *105* (22), 9982-9985.

5.   Adamo, C.; Barone, V., Toward Reliable Density Functional Methods without Adjustable Parameters: The PBE0 Model. *The Journal of chemical physics* **1999,** *110* (13), 6158-6170.

6.   Perdew, J. P.; Parr, R. G.; Levy, M.; Balduz, J. L., Density-Functional Theory for Fractional Particle Number: Derivative Discontinuities of the Energy. *Physical Review Letters* **1982,** *49* (23), 1691-1694.

7.   Ambrosio, F.; Wiktor, J.; De Angelis, F.; Pasquarello, A., Origin of Low Electron–Hole Recombination Rate in Metal Halide Perovskites. *Energy & Environmental Science* **2018,** *11* (1), 101-105.

8.   Perdew, J. P.; Burke, K.; Ernzerhof, M., Generalized Gradient Approximation Made Simple. *Physical Review Letters* **1996,** *77* (18), 3865-3868.

9.   Alkauskas, A.; Broqvist, P.; Pasquarello, A., Defect Energy Levels in Density Functional Calculations: Alignment and Band Gap Problem. *Physical Review Letters* **2008,** *101* (4), 046405.

10.   Alkauskas, A.; Broqvist, P.; Pasquarello, A., Defect Levels Through Hybrid Density Functionals: Insights and Applications. *Physica Status Solidi (b)* **2011,** *248* (4), 775-789.

11.   Komsa, H.-P.; Broqvist, P.; Pasquarello, A., Alignment of Defect Levels and Band Edges through Hybrid Functionals: Effect of Screening in the Exchange Term. *Physical Review B* **2010,** *81* (20), 205118.

12.   Ambrosio, F.; Miceli, G.; Pasquarello, A., Redox Levels in Aqueous Solution: Effect of van der Waals Interactions and Hybrid Functionals. *The Journal of Chemical Physics* **2015,** *143* (24), 244508.

13.   Alkauskas, A.; Broqvist, P.; Devynck, F.; Pasquarello, A., Band Offsets at Semiconductor-Oxide Interfaces from Hybrid Density-Functional Calculations. *Physical Review Letters* **2008,** *101* (10), 106802.

14.   Zheng, K.; Abdellah, M.; Zhu, Q.; Kong, Q.; Jennings, G.; Kurtz, C. A.; Messing, M. E.; Niu, Y.; Gosztola, D. J.; Al-Marri, M. J.; Zhang, X.; Pullerits, T.; Canton, S. E., Direct Experimental Evidence for Photoinduced Strong-Coupling Polarons in Organolead Halide Perovskite Nanoparticles. *The Journal of Physical Chemistry Letters* **2016,** *7* (22), 4535-4539.

15.   Miceli, G.; Chen, W.; Reshetnyak, I.; Pasquarello, A., Nonempirical Hybrid Functionals for Band Gaps and Polaronic Distortions in Solids. *Physical Review B* **2018,** *97* (12), 121112.

16.   Nguyen, N. L.; Colonna, N.; Ferretti, A.; Marzari, N., Koopmans-Compliant Spectral Functionals for Extended Systems. *Physical Review X* **2018,** *8* (2), 021051.

17.   Halgren, T. A.; Lipscomb, W. N., The Synchronous-Transit Method for Determining Reaction Pathways and Locating Molecular Transition States. *Chemical Physics Letters* **1977,** *49* (2), 225-232.

18.   Nosé, S., A unified formulation of the constant temperature molecular dynamics methods. *The Journal of Chemical Physics* **1984,** *81* (1), 511-519.

19.   Hoover, W. G., Canonical dynamics: Equilibrium phase-space distributions. *Physical Review A* **1985,** *31* (3), 1695-1697.

20.   Stoumpos, C. C.; Malliakas, C. D.; Kanatzidis, M. G., Semiconducting Tin and Lead Iodide Perovskites with Organic Cations: Phase Transitions, High Mobilities, and Near-Infrared Photoluminescent Properties. *Inorganic Chemistry* **2013,** *52* (15), 9019-9038.